Binding of Dioxygen to Non-Metal Sites in Proteins: Exploration of the Importance of Binding Site Size versus Hydrophobicity in the Copper Amine Oxidase from *Hansenula polymorpha*†

Yoshio Goto‡ and Judith P. Klinman*

Department of Chemistry and Department of Molecular and Cell Biology, University of California, Berkeley, California 94720

Received July 8, 2002

ABSTRACT: Copper amine oxidases (CAOs) contain 2,4,5-trihydroxyphenylalanyl quinone (TPQ) and a copper ion in their active sites, catalyzing amine oxidation to aldehyde and ammonia concomitant with the reduction of molecular oxygen to hydrogen peroxide. Kinetic studies on the CAO from bovine serum (BSAO) [Su and Klinman (1999) *Biochemistry 37*, 12513−12525] and the recent reports on the cobalt substituted form of the enzyme from *Hansenula polymorpha* (HPAO) [Mills and Klinman (2000) *J. Am. Chem. Soc*. *122*, 9897−9904, and Mills et al. (2002) *Biochemistry*, *41*, 10577−10584] support pre-binding of molecular oxygen prior to a rate-limiting electron transfer from the reduced form of TPQ (*p*-aminohydroquinone form) to dioxygen. Although there is significant sequence homology between BSAO and HPAO, $k_{cat}/K_m(O_2)$ for BSAO under the optimal condition is one order of magnitude lower than that for HPAO. From a comparison of amino acid sequences for BSAO and HPAO, together with the X-ray crystal structure of HPAO, a plausible dioxygen pre-binding site has been identified that involves Y407, L425, and M634 in HPAO; the latter two residues are altered in BSAO to A490 and T695. To determine which of these residues plays a greater role in dioxygen chemistry, $k_{cat}/K_m(O_2)$ was determined in HPAO for the M634 → T and L425 → A mutants. The L425 → A mutation does not alter $k_{cat}/K_m(O_2)$ to a large extent, whereas the M634 → T decreased $k_{cat}/K_m(O_2)$ by one order of a magnitude, creating a catalyst that is similar to BSAO. A series of mutants at M634 (to F, L, and Q) were, therefore, prepared in HPAO and characterized with regard to $k_{cat}/K_m(O_2)$ as a function of pH. Structure reactivity correlations show a linear relationship of rate with side chain volume, rather than hydrophobicity, indicating that dioxygen reactivity increases with the bulk of the residue at position 634. This site also shows specificity for O_2, in relation to the co-gas N_2, since substitution of the inert gas N_2 by either Ar or He has no effect on measured rates. In particular, He gas is expected to have little affinity for protein at 1 atmospheric pressure, implying little or no binding by N_2 as well.

Many enzymatic systems utilize dioxygen as an oxidant. The manner whereby these enzymes catalyze O_2 activation, in general to free radical intermediates, while avoiding self-inactivation is of great interest (*1*). Investigations of the reaction of the copper amine oxidases (CAOs)[1] with molecular oxygen have revealed a number of unexpected mechanistic features. This enzyme contains a tyrosine residue-derived 2,4,5-trihydroxyphenylalanyl quinone (TPQ) moiety and a copper ion ligated by three histidine imidazoles and two waters in the active site (cf. *2* and refs therein). The catalytic cycle of the CAO consists of two half-reactions, with the properties of a ping-pong mechanism: in the reductive half-reaction, the oxidized form of TPQ oxidizes a substrate primary amine to the corresponding aldehyde while transferring its amino group to cofactor. The resulting reduced form of the cofactor (an aminoquinol) is then reoxidized by O_2 to produce hydrogen peroxide in the oxidative half-reaction (*3*) (Scheme 1). Extensive kinetic characterizations of the oxidative half reaction in CAOs from bovine serum (BSAO) (*4*) and *Hansenula polymorpha* (HPAO) (*5, 6*), which include pH dependencies, solvent and oxygen-18 kinetic isotope effects, and the effect of solvent viscosity on rate, have led to a model in which O_2 binds and reacts initially at a site that is "off" the active site copper ion (Scheme 1). According to this model, the metal ion plays the role of stabilizing and binding reduced oxygen intermediates, without a need for a cycling of metal between the cupric and cuprous states. Since a general strategy for oxygen capture in metalloenzymes is based on redox chemistry at the metal center, i.e., $M^{n-1} + O_2 \rightarrow M^n{-}O_2^{-}\bullet$ (*7*), this type of nonredox dioxygen binding is quite unique.

Strong support for the mechanism of Scheme 1 comes from metal replacement studies, in which the cobaltous form of HPAO indicates high levels of enzyme activity, compa-

† This work was supported by grants from the National Institutes of Health (GM 39296 and GM 25765).

* To whom correspondence should be addressed. Phone: 510-642-2668. Fax: 510-643-6232. E-mail: klinman@socrates.berkeley.edu.

‡ Current address: ERATO Nanospace Project, Japan Science and Technology Corporation, c/o Museum of Emerging Science and Innovation, Research Building 4F, 2−41 Aomi, Koto-ku, Tokyo 135-0064, Japan.

[1] Abbreviations: CAO, copper amine oxidase; TPQ, 2,4,5-trihydroxyphenylalanyl quinone; HPAO, copper amine oxidase from *Hansenula polymorpha*; BSAO, copper amine oxidase from bovine serum; WT-HPAO, wild-type HPAO.

10.1021/bi0204591 CCC: $22.00
Published on Web 10/23/2002

Scheme 1: Proposed Mechanism for the Oxidative Half Reaction of the Amine Oxidases[a]

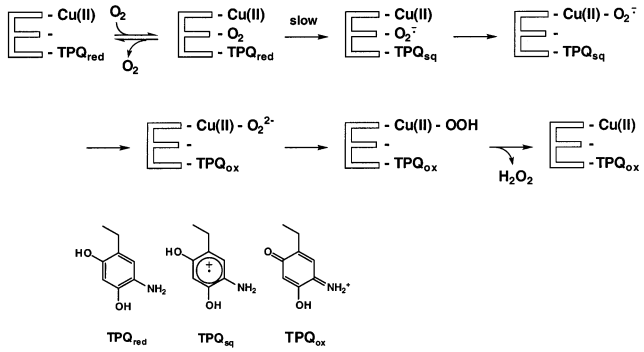

[a] The structures for the three forms of TPQ in cycle are also shown: the reduced form, TPQ_{red}; the semiquinone form, TPQ_{sq}; and oxidized form, TPQ_{ox}, with product ammonia bound as a Schiff base.

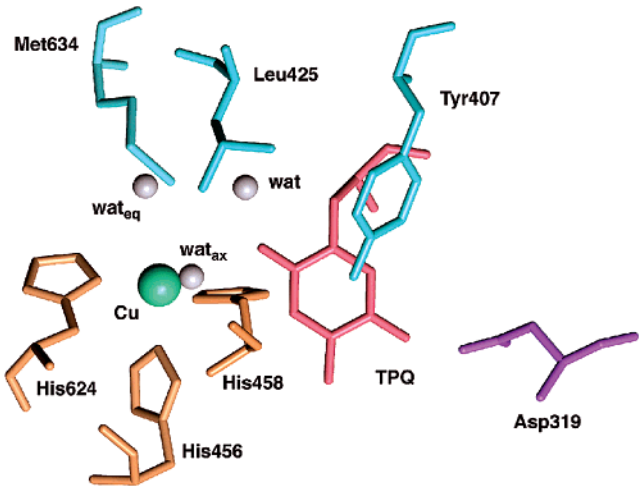

FIGURE 1: Active site structure of HPAO [Ref (*2*)]. The proposed O_2 binding site is composed of the residues in blue, Y407, L425, and M634. Waters and the copper ion are depicted as spheres.

rable to wild-type enzyme (*5*). In very recent studies, a detailed mechanistic comparison between copper- and cobalt-containing forms of HPAO indicates very similar kinetic and chemical mechanisms, with the major difference being a decrease in O_2 affinity to the cobalt form of enzyme. This latter property is ascribed to a large increase in the pK_a for water bound to cobalt, with a concomitant alteration in the net charge on the metal site that adjoins the O_2 binding site (*6*).

A putative O_2 binding site near the active site copper has been located by inspection of the available X-ray crystal structure for HPAO (*2*) and by structural and sequence alignment of HPAO with other CAOs (*8*). In the case of HPAO, a pocket that is lined by hydrophobic residues has been identified: Met 634, Leu 425, and Tyr 407 (Figure 1). The mammalian CAO, BSAO, shows a Met-to-Thr substitution at position 695 and a Leu-to-Ala substitution at position 490 (*4*). As described herein, we have performed site-specific mutagenesis on HPAO, showing that Met 634 is a key determinant of O_2 affinity. Mutation of this residue to the Thr found in BSAO has the effect of converting the kinetic properties of HPAO into those of BSAO. By subsequent replacement of Met 634 with a series of amino acid side chains that vary in size and hydrophobicity, it has been possible to analyze the factors that control O_2 reactivity.

These studies indicate that the nature of the side chain at position 634 in HPAO affects both the pK_as and limiting rates for the oxidative half reaction [defined by $k_{cat}/K_m(O_2)$]. We propose that hydrophobicity is the key factor in altering active site pK_as, whereas the limiting rate constants correlate with side chain size. Surprisingly, the same rate for O_2 reactivity is seen, independent of whether O_2 concentration is controlled by addition of nitrogen, argon, or helium as an inert gas. The possible implications of this unexpected result are discussed.

MATERIALS AND METHODS

Materials. All chemical materials were purchased from commercial providers and used without further purification, except as noted. Methylamine hydorochloric acid salt was recrystallized from ethanol. Protocatechuate dioxygenase was purchased from Sigma-Aldrich. Restriction enzymes were purchased from New England BioLabs Inc.

*Enzyme Preparation.*Wild-type (WT) and mutant forms of HPAO were expressed in *Saccharomyces cerevisiae* and purified as described by Plastino et al. (*9*), with the slight modification of Mills and Klinman (*5*). Site-directed mutagenesis was performed by using Cameleon or QuickChange Site Directed Mutagenesis kits from Stratagene. Selection of mutant versus WT DNA in pDB20 was accomplished with the unique *Aat*III (for L425A) or *Eco*RI (for M634 mutants) site by silent mutation, using synthetic oligonucleotide primers (Operon Technologies Inc.): 5′-GCC ATC AGA CTC GAC ATC AGA **GC**C ACC GG**A** ATT CTG AAC ACG TAC-3′ for L425A and 5′-CCT GAG GAC TTC CCA TTG **MMM** CC**G** GCC GAG CCT ATC ACC-3′ for M634Xs, where **MMM** = **TTC**, **CC**G, **AC**G, and **CA**G for M634F, M634L, M634T, and M634Q, respectively. The mutated nucleotides are shown in boldface and the selection site underlined**.** Plasmid purification steps were performed with kits and materials purchased from Qiagen, Inc. Prepared mutant genes were sequenced in the DNA sequencing facility of the University of California, Berkeley. Protein concentration was determined by Bradford Protein Assay (Bio-Rad) using bovine serum albumin as a standard. The concentration of active enzyme was determined by phenylhydrazine derivatization of TPQ as described by Mills et al. (*6*).

Steady-State Kinetic Assays. For the ping-pong mechanism of CAO, k_{cat}/K_m of the second substrate is independent of parameters from the first half-reaction (*10*). In the determination of the k_{cat}/K_m(amine) and $k_{cat}/K_m(O_2)$ parameters, the alternate substrate was saturated, i.e., at a concentration at least 10 times higher than K_m (concentrations of 3−18 mM for methylamine, and ∼1 mM for O_2). The initial velocity of reaction was measured by monitoring dioxygen consumption with a Yellow-Springs oxygen electrode system at 25 °C, as described in Su and Klinman (*4*), and plotted against the concentration of the substrate; these plots were fitted to the Michaelis−Menten equation by nonlinear regression. Assay solutions were as follows: for pH 5.5, 100 mM potassium acetate buffer; for pH 6−8, potassium phosphate; for pH above 8, potassium pyrophosphate or sodium carbonate. Ionic strength was adjusted to 300 mM by the addition of potassium chloride. The parameters k_{cat}, k_{cat}/K_m(amine), and $k_{cat}/K_m(O_2)$ were plotted against pH in log scale and fitted to one of the following equations (*6*, *11*):

$$\log(x) = \log(x)_{max} - \log(1 + 10^{pK_{a1}-pH} + 10^{pK_{a1}+pK_{a2}-2pH} + 10^{pH-pK_{a3}}) \quad (1)$$

$$\log(x) = \log(x)_{max} - \log(1 + 10^{pK_{a1}-pH} + 10^{pH-pK_{a2}}) \quad (2)$$

$$\log(x) = \log(x)_{max} - \log(1 + 10^{pK_{a1}-pH} + 10^{pK_{a1}+pK_{a2}-2pH}) \quad (3)$$

$$\log(x) = \log(x)_{max} - \log(1 + 10^{pK_{a1}-pH}) \quad (4)$$

The kinetic measurements for BSAO in Su and Klinman (*4*) have been converted to units of M^{-1} and s^{-1} on the basis of the activity at the concentration of the enzyme determined by phenylhydrazine derivatization assay (*12*).

Viscosity Effect on $k_{cat}/K_m(O_2)$. The viscosity effect on $k_{cat}/K_m(O_2)$ was measured at pH 7.2 (M634F), pH 7.8 (WT, M634T, and M634Q) and pH 8.0 (M634L) at 25 °C [this study and ref *12*]. Glucose was chosen as a viscosogen in the study of BSAO by Su and Klinman (*4*); however, glucose appeared to have an inhibitory effect on $k_{cat}/K_m(O_2)$ in the case of HPAO, so that sucrose or glycerol was used instead. The relative viscosity for viscosogen-containing solutions was determined by using an Ostwald viscometer at 25 °C. Viscosogen may affect the solubility of O_2 in solution; thus, the O_2 concentration in the viscous solution was calibrated with a protocatechuate 3,4-dioxygenase assay in which protocatechuic acid is used as substrate; the end point of O_2 consumption was observed by O_2 electrode system (*13*). The relative viscosity reported is an average of five determinations at each viscosogen concentration. Data were fitted to eq 5 (*4*, *6*), where $(k_{cat}/K_m)°$ is in the absence of viscosogen and $\eta/\eta°$ is the relative viscosity of the solution. The slope of the line, *S*, reflects the degree of viscosity dependence.

$$\frac{(k_{cat}/K_m)°}{(k_{cat}/K_m)} = S\left(\frac{\eta}{\eta°} - 1\right) + 1 \quad (5)$$

RESULTS AND DISCUSSION

Conversion of Residues in the O_2 Binding Pocket of HPAO to Those of BSAO. The oxidative half reaction of the copper amine oxidases (CAOs) involves reaction of molecular oxygen with the reduced aminoquinol form of the active site TPQ cofactor to produce oxidized cofactor and hydrogen peroxide:

$$\text{E-TPQ}_{red} + O_2 \rightarrow \text{E-TPQ}_{ox} + H_2O_2 \quad (6)$$

In this laboratory, the reaction in eq 6 has been characterized in detail for enzymes from *Hansenula polymorpha* (HPAO) and bovine serum (BSAO), showing very similar chemical mechanisms together with 1 order of magnitude decrease in $k_{cat}/K_m(O_2)$ for BSAO at limiting pH values (*4*, *6*).

With the identification of a likely O_2 binding site in HPAO (Figure 1), we wished to examine whether residues in this pocket were the origin of the reduced rate for $k_{cat}/K_m(O_2)$ with BSAO. Although an X-ray structure is not yet available for a mammalian CAO, structures have been determined for enzymes from a number of sources (*E. coli.*, *14*, *A. globiformis*, *15*, and pea seedlings amine oxidase, *16*, in addition to HPAO, *2*). Through a comparison of the existing three-dimensional structures, together with primary sequence alignments for copper amine oxidases from 10 sources (*8*), two residues were identified in BSAO as the analogue of the Leu 425 and Met 634 in the proposed O_2 binding pocket of HPAO; these are Ala 490 and Thr 695 (*2*).

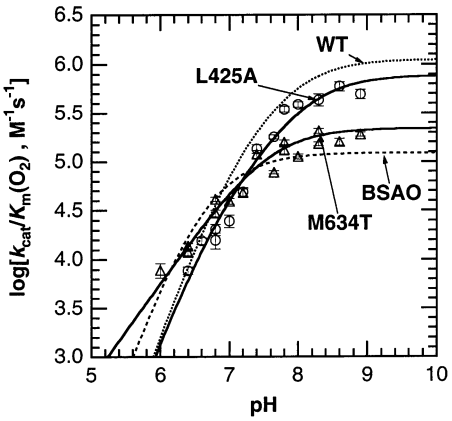

FIGURE 2: Comparison of pH profiles for $k_{cat}/K_m(O_2)$ for mutants of HPAO in comparison to BSAO. L425A (circle) and M634T (triangle) in comparison with WT HPAO [ref *6*] (dotted line) and BSAO [refs *4* and *12*] (broken line). Plots for L425A (and WT and BSAO) are fitted with two-pK_a model (eq 3 in text), while the one for M634T is fitted with the one-pK_a model (eq 4 in text).

Table 1: Comparison of Kinetic Parameters for HPAO, Mutated at the O_2 Binding Site to Resemble BSAO

enzyme form	$[k_{cat}/K_m(O_2)]_{max}$[a] ($M^{-1}s^{-1}$)	pK_{a1}	pK_{a2}
WT[b]	$(1.0 \pm 0.2) \times 10^6$	6.9 ± 0.1	7.9 ± 0.2
L425A	$(7.7 \pm 0.1) \times 10^5$	6.5 ± 0.3	8.2 ± 0.2
M634T	$(1.9 \pm 0.3) \times 10^5$	7.5 ± 0.1	—[c]
BSAO[d]	1.2×10^5	6.2 ± 0.3	7.0 ± 0.2

[a] Extrapolated to the maximum limiting rate from fitting of eq 3 or 4 to plots of $k_{cat}/K_m(O_2)$ vs pH. Data were collected between pH 6 and 9. [b] Ref *6*. [c] Only a single pK_a was observed. [d] Refs *4* and *12*.

Following the preparation of the L425A and M634T mutants in HPAO, initial rate parameters were collected as a function of O_2 concentration to obtain $k_{cat}/K_m(O_2)$. The $k_{cat}/K_m(O_2)$ parameters, collected between pH 6 and 9, yielded the data shown in Figure 2 and the parameters in Table 1. In the case of the L425A mutant, only a small deviation from the WT HPAO was seen with regard to the limiting rate constant and pK_a values. By contrast, conversion of Met 634 to Thr results in a limiting rate for $k_{cat}/K_m(O_2)$ that is almost superimposable on that for BSAO. With the available data, we were only able to identify a single pK_a that controls $k_{cat}/K_m(O_2)$ for M634T; this lies between the two pK_as that have been determined for WT-HPAO. This alteration in detectable pK_a values will be discussed in greater detail below. Importantly, these studies identify the Met 634 as an important side chain determinant in oxygen reactivity.

Structure−Reactivity Investigation of Position 634 in HPAO. A series of mutants were prepared at position 634 in HPAO to examine the factors that impact O_2 binding and reactivity. With the understanding that O_2 dissolves more readily in organic solvents than water (*17*), the side chains were chosen based on their relative hydrophobicity, as defined by their free energy of transfer from water to organic solvent (*18* cf. *19* and refs. therein). Two strongly hydrophobic residues (Phe, and Leu, with free energies of transfer

Table 2: Effects of Alteration in Position 634 in HPAO on k_{Cat} and k_{Cat}/K_m(Amine)

AA residue at 634	$[k_{cat}/K_m(amine)]_{max}$[a] ($M^{-1}$ s^{-1})	$[k_{cat}]_{max}$[a] (s^{-1})
Met (WT)[b]	3.2×10^5	7.8
Phe	$(1.2 \pm 0.1) \times 10^5$	3.6 ± 0.6
Leu	$(2.1 \pm 0.1) \times 10^5$	5.8 ± 1.1
Thr	$(1.6 \pm 0.1) \times 10^5$	3.5 ± 0.1
Gln	$(2.7 \pm 0.1) \times 10^5$	6.0 ± 0.1

[a] Extrapolated to the maximum limiting rate from fitting of eq 1 or 2 to plots of $k_{cat}/K_m(O_2)$ vs pH. Data were collected between pH 6 and 9. [b] Refs *6* and *20*.

of 3.7 and 2.8 kcal/mol), one moderately hydrophobic residue (Thr, with a free energy transfer of 1.2 kcal/mol), and one hydrophilic residue (Gln, with a free energy of transfer of −4.1 kcal/mol) were prepared and characterized. These can be compared to Met in WT-HPAO, with a free energy transfer of 3.4 kcal/mol.

Prior to examining the data for the oxidative half reaction, as measured by $k_{cat}/K_m(O_2)$, the effects of mutations at position 634 on the parameters k_{cat}/K_m(amine) and k_{cat} were analyzed. In particular, the reductive half reaction, defined by k_{cat}/K_m(amine), serves as an important control, since the site at which amine binds and reacts is expected to lie on the opposite side of the cofactor from that of O_2 binding and reactivity. As summarized in Table 2, the values for $[k_{cat}/K_m(amine)]_{max}$ determined by eq 2 (under optimal condition) undergo less than a 3-fold change among the mutants, with the fastest rate being observed with WT-HPAO. Studies of substrate deuterium isotope effects with WT enzyme indicate that substrate oxidation is partially rate-determining, with substrate binding also implicated as a slow step (*20*). The small, observed decreases in k_{cat}/K_m (amine) among the mutants appear to be uncorrelated with either side chain hydrophobicity or side chain size (see discussion below).

The effects of mutation at 634 on values for k_{cat}, determined by eq 1 (*6*), at their pH optima, are also summarized in Table 2. Analogous to k_{cat}/K_m(amine), k_{cat} for WT is very close in magnitude to those for M634L and M634Q. The slightly slower mutants, M634T and M634F, are only about 2-fold reduced in rate, and once again, no discernible trend is detected with regard to the nature of the side chain. The failure to see a substrate deuterium isotope effect on k_{cat} with WT-HPAO, together with the demonstrated accumulation of the reduced aminoquinol form of cofactor during steady-state turnover with saturating amine and O_2, has led to the conclusion that the first electron transfer from reduced cofactor to O_2 is largely rate-determining (*5*, *6*). This is likely, though not proven, to be the case with the mutants, suggesting that the chemistry that occurs between bound O_2 and reduced cofactor is not highly dependent on the nature of side chain 634.

The kinetic analyses of k_{cat} and k_{cat}/K_m(amine) were focused on obtaining limiting rate parameters and not pK_a values. Of potential mechanistic interest are the acidic pK_as that control the ionization of the active site base [seen in k_{cat}/K_m(amine)] and the ionization of reduced cofactor and a metal-bound water (seen in k_{cat}). In the case of the acidic pK_a in k_{cat}/K_m(amine), which has been assigned to the active site base, a similar value (from 8.1 to 8.4) was found among WT and mutant enzymes (data not shown). Analysis of the

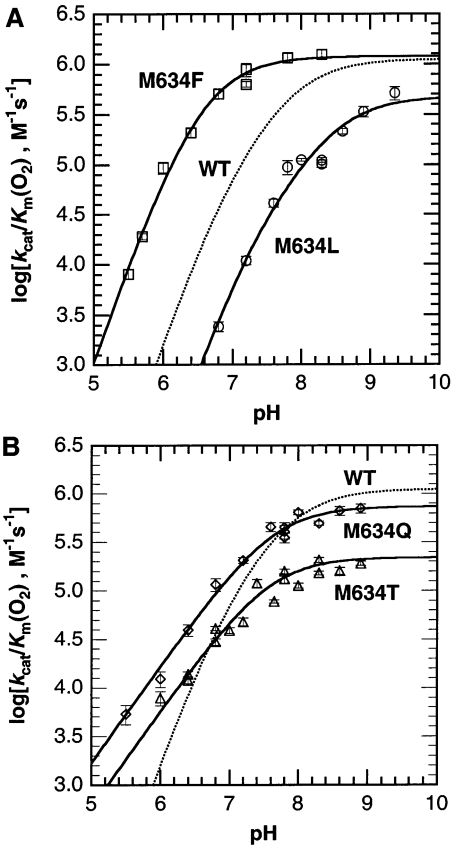

FIGURE 3: Effects of mutagenesis at M634 in HPAO on $k_{cat}/K_m(O_2)$. (A) pH profiles of M634F (rectangle) and M634L (circle) in comparison with WT HPAO [Ref (*6*)] (dotted line). Plots for the mutants are fitted to a two-pK_a model (eq 3 in text). (B) pH profiles of $k_{cat}/K_m(O_2)$ in M634T (triangle) and M634Q (diamond). Plots for the mutants are fitted to a one-pK_a model (eq 4 in text).

Table 3: Parameters for $k_{Cat}/K_m(O_2)$ with HPAO Variants Mutated at Position 634

AA residue at 634	$[k_{cat}/K_m(O_2)]_{max}$[a] ($M^{-1}s^{-1}$)	pK_{a1}	pK_{a2}
Met (WT)[b]	$(1.0 \pm 0.2) \times 10^6$	6.9 ± 0.1	7.9 ± 0.2
Phe	$(1.2 \pm 0.1) \times 10^6$	6.2 ± 0.2	6.8 ± 0.2
Leu	$(4.7 \pm 1.0) \times 10^5$	7.1 ± 0.3	8.6 ± 0.2
Thr	$(1.9 \pm 0.3) \times 10^5$	7.5 ± 0.1	−[c]
Gln	$(7.4 \pm 0.7) \times 10^5$	7.6 ± 0.1	−[c]

[a] Extrapolated to the maximum limiting rate from fitting of eq 3 or 4 to plots of $k_{cat}/K_m(O_2)$ vs pH. Data were collected between pH 5.5 and 10. [b] Ref *6*. [c] Only a single pK_a was observed.

acidic pK_as in k_{cat} among the mutants was not attempted, as this requires deconvolution of two ionizing residues and a larger number of data points than were available.

Turning to the oxidative half reaction, rates were obtained at a single pH as a function of dioxygen concentration to yield the second-order parameter $k_{cat}/K_m(O_2)$; this was then repeated in the range of pH 5.5−9.4. The data for M634F and M634L are shown in Figure 3A, and those for M634Q are presented in Figure 3B, together with the previously determined analysis of M634T. Limiting rate constants at high pH and pK_a values defined by the pH profiles are summarized in Table 3.

The effect of side chain replacement on the limiting rate constants was first analyzed as a function of side chain hydrophobicity, and the results are shown in Figure 4A.

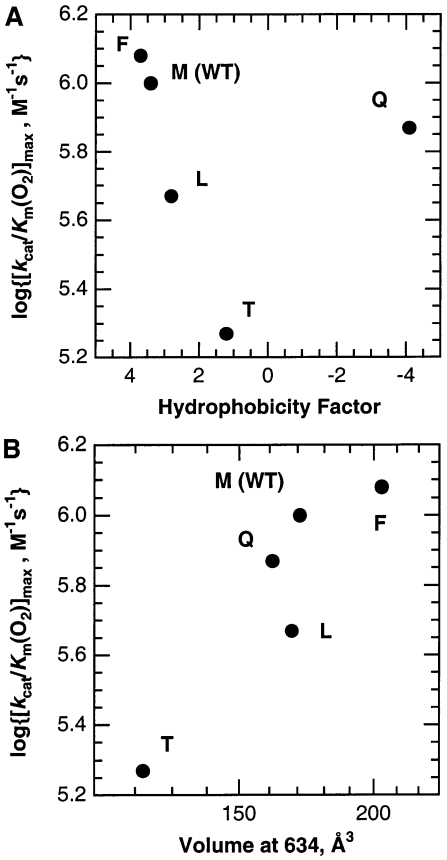

FIGURE 4: Structure function correlations at position M634 in HPAO. The letter indicates the amino acid at position 634. (A) Relationship between $k_{cat}/K_m(O_2)$ and side chain hydrophobicity. (B) Relationship between $k_{cat}/K_m(O_2)$ and side chain volume.

While a trend in rate for three of the mutant enzymes lies on a line with the data for WT-HPAO, the Met-to-Gln mutant is a dramatic outliner. Up to this point, our expectation had been that dioxygen, with its greater solubility in organic solvents than water, would show a tighter binding (*17*) and, hence, greater $k_{cat}/K_m(O_2)$ with enhanced hydrophobicity of its binding site. Although we considered the possibility that the M634Q mutant was aberrant for reasons that were due to structural changes outside the dioxygen pocket, it appeared more likely that a factor different from the free energy of transfer to organic solvent was determining O_2 reactivity.

A second correlation was then attempted on the basis of the size of the amino acid side chain. As shown in Figure 4B, the volume of the side chain (*21*) shows a consistent correlation with $k_{cat}/K_m(O_2)$ for all four mutants as well as the WT-HPAO. Thus, the correlation in Figure 4B suggests that the size of the side chain impacts the ability of O_2 to bind in a catalytically viable mode within its pocket. We note that the largest mutant, M634F, actually shows a rate that is slightly faster than that for the WT-HPAO; this is a rare observation, in which site-specific mutagenesis produces a form of enzyme with increased rate relative to the WT.

It is noteworthy that the size (or shape) of the binding site is more important for the rate of electron transfer than the hydrophobic interaction between the protein structure and dioxygen. How can it be that spaciousness, or packing at the O_2 binding site, affects $k_{cat}/K_m(O_2)$? The parameter $k_{cat}/K_m(O_2)$ for WT-HPAO has been shown to reflect a rate-determining electron transfer from the reduced TPQ to O_2 that has pre-bound to its site. To examine whether a similar rate-limiting step was operating for the M634 mutants, the rate of $k_{cat}/K_m(O_2)$ was examined in the presence of the viscosogen glycerol or sucrose. In no instance was there a diminution of rate with increasing viscosogen (data not shown), supporting a similar rate-limiting step for each of the mutants as for WT. Since electron-transfer rate is expected to be controlled by the distance between donor and acceptor (*22*), precise positioning of the bound O_2, as determined by side chain packing, could have provided the explanation for the correlation shown in Figure 4B. However, in WT-HPAO, both k_{cat} and $k_{cat}/K_m(O_2)$ are concluded to be controlled by a similar rate-limiting electron-transfer step (*6*). As shown in Table 2, mutants at position 634 affect k_{cat} very little, leading us to attribute the major impact of side chain size on the binding of O_2 into the enzyme pocket (Figure 1). This point is addressed further in the section "Discrimination against Gases at the Dioxygen Site of HPAO".

We also attempted to understand the observed trends in the kinetically determined pK_a values for $k_{cat}/K_m(O_2)$ among the mutants (Table 3). From studies of the WT-HPAO and a cobalt-substituted form of enzyme, the pK_as that control the ionization of the protonated aminoquinol of TPQ to its neutral form and the ionization of a copper-bound water have been assigned as pK_{a1} = 6.9 and pK_{a2} = 7.9, respectively (*6*). As seen in Table 3, two mutants (M634T and M634Q) indicate only a single pK_a in the experimental range of pH values. Three possibilities were considered for this observation: first, that both ionizing residues had coalesced to a single pK_a; second, that one pK_a has been reduced to below the lowest pH studied; and third, that a single pK_a has been elevated above the highest pH value studied.

The first possibility was ruled out from the finding of slopes close to unity in pH rate plots. From structural studies, the principal control of the elevated pK_a for the aminoquinol form of TPQ, relative to a model compound in solution (pK_a 5.9) (*23*), is likely to come from an ionic interaction with the active site, carboxylate base (Asp 319, in Figure 1) that resides in the substrate binding pocket on the opposite side of the cofactor from the proposed O_2 binding pocket. From the analysis of k_{cat}/K_m(amine), we have found that the pK_a for the active site base is largely unaffected by the side chain at position 634 (see above). Thus, it appeared far more likely that the ionization of the copper water would be affected by mutations in the dioxygen binding site. An important observation is that the M634Q mutant has activity approaching WT-HPAO, in contrast to the effect of cobalt substitution in HPAO where an elevated pK_a leads to a dramatic increase in K_m for O_2 and resulting decrease in $k_{cat}/K_m(O_2)$. We therefore suggest an opposite effect of M634Q and M634T from that of cobalt substitution, i.e., a reduction in the pK_a for the metal-bound water below the experimental pH range. The distinguishing feature of both M634T and M643Q from WT and the other mutants is their capacity to enter into hydrogen bonding. It is the potential for hydrogen bonding that may impact the ability to form and stabilize $Cu^{2+}-OH$ better than in the case of WT-HPAO. Future studies that are focused on the direct detection of the ionization state of the copper-water may provide confirmation of this proposal.

From the above arguments, the single observed pK_a for M634T and M634Q is tentatively assigned to that of reduced cofactor and, thus, compared to pK_{a1} for WT-HPAO and the

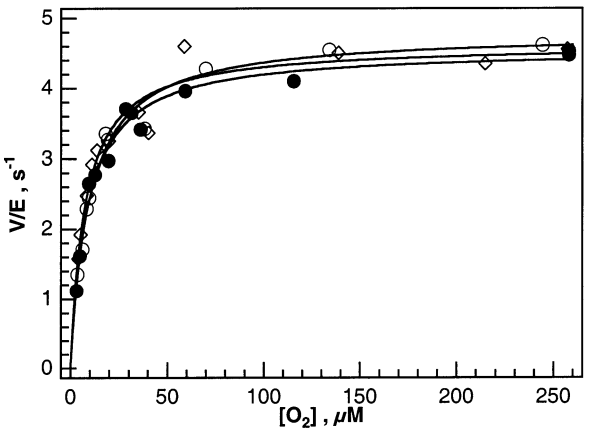

FIGURE 5: Plots of initial velocity of enzyme, normalized to enzyme concentration, vs $[O_2]$ for WT HPAO in the presence of N_2 (closed circle), Ar (open circle), or He (diamond) as the co-gas in the atmosphere (total pressure = 1 atm). Kinetic parameters k_{cat} (s^{-1}) and $K_m(O_2)$ (μM) under N_2, Ar, and He are (4.6 ± 0.1, 9 ± 1), (4.8 ± 0.1, 10 ± 1), and (4.6 ± 0.1, 7 ± 1), respectively. The reactions were performed in 100 mM potassium phosphate buffer, pH 7.8, ionic strength 300 mM, at 25 °C, in the presence of 6 mM substrate methylamine.

other mutants. With the exception of M634F, the values for this pK_a (Table 3) lie in a fairly narrow range between 6.9 and 7.6. This appears consistent with the view that mutants in the O_2 pocket have a relatively small effect on the ionization of the aminoquinol, analogous to their small effect on the pK_a for the proximal active site base. In an earlier study, substitution of the active site copper with cobalt was similarly found to leave the pK_a for aminoquinol almost unaltered (6.7 vs 6.8 of WT) (*6*).

One striking feature of the data in Table 2 is the trend in pK_as for M643F in relation to WT-HPAO. The observation that both pK_as decrease by ca. 1 pH unit may reflect structural shifts that affect the position of cofactor and the positioning of the water networks known to be at the active site. Structural comparison of M643F to WT-HPAO is expected to be quite informative.

Discrimination against Gases at the Dioxygen Site of HPAO? The data obtained for mutants at position 634 in HPAO implicate a role for amino acid side chain size in controlling the magnitude of $k_{cat}/K_m(O_2)$. Since k_{cat} is affected very little (Table 2), the data point toward a role for side chain size in O_2 binding. With this observation, we became very interested in the possibility of discrimination between O_2 and other atmospheric gases at the gaseous site. The chemical literature documents molecular sieves that have been designed to distinguish between O_2 (with a molecular length of 3.9 Å) from N_2 (with a molecular length of 4.1 Å) (*24*).

In particular, we wished to know whether the site for O_2 in HPAO had been engineered to allow for such high specificity that N_2 could be excluded. If this is not the case, then $k_{cat}/K_m(O_2)$ studies, conducted in N_2/O_2 mixtures, are expected to be affected by competition between N_2 and O_2. This possibility was tested by remeasuring $k_{cat}/K_m(O_2)$ in the presence of either He or Ar as the inert gas (Figure 5). As shown, the measured rates are indistinguishable, independent of whether N_2, Ar, or He is added to control O_2 concentrations. One possible explanation is that all four gases show the same affinity for the O_2 site, implicating equal competition between O_2 and either N_2, He, or Ar. However, given the anticipated very low affinity at atmospheric pressure of the small, inert He, with its extremely weak van der Waals interactions *(25)*, it is far more likely that the data in Figure 5 implicate negligible binding of Ar and N_2 as well. This is an intriguing result and may indicate a capacity for proteins to generate highly specific, off-metal dioxygen binding sites.

CONCLUSIONS

A hydrophobic pocket has been proposed to pre-bind O_2 in the oxidative half reaction of the copper amine oxidase. Site-specific mutagenesis at two of the three residues within this pocket indicates M634 (in HPAO) as an important determinant of reactivity. Measurement of $k_{cat}/K_m(O_2)$ for a series of mutants, M634X, indicates a linear correlation between $k_{cat}/K_m(O_2)$ and side chain volume. This effect is attributed to an impact of side chain bulk on O_2 affinity for the enzyme. The finding that the rate of O_2 consumption is identical in the presence of N_2, Ar and He as co-gas provides support for specificity in O_2 binding as well.

ACKNOWLEDGMENT

We thank Dr. Qiaojuan J. Su for her preliminary experiments on HPAO mutation and Amy Olgin for the viscosity measurements.

REFERENCES

1. Klinman, J. P. (2001) *J. Biol. Inorg. Chem. 6*, 1−13.
2. Li, R. B., Klinman, J. P., and Mathews, F. S. (1998) *Structure 6*, 293−307.
3. Klinman, J. P. (1996) *J. Biol. Chem. 271*, 27189−27192.
4. Su, Q., and Klinman, J. P. (1998) *Biochemistry 37*, 12513−12525.
5. Mills, S. A., and Klinman, J. P. (2000) *J. Am. Chem. Soc. 122*, 9897−9904.
6. Mills, S. A., Goto, Y., Su, Q. J., Plastino, J., and Klinman, J. P. *Biochemistry 41*, 10577−10584.
7. Ho, R. Y. N., Liebman, J. F., and Valentine, J. S. (1995) in *Active Oxygen in Biochemistry* (Valentine, J. S., Foote, C. S., Greenberg, A., and Liebman, J. F., Eds.) pp 1−36, Blackie Academic & Professional, London.
8. Tipping, A. J., and McPherson, M. J. (1995) *J. Biol. Chem. 270*, 16939−16946.
9. Plastino, J., Green, E. L., Sanders-Loehr, J., and Klinman, J. P. (1999) *Biochemistry 38*, 8204−8216.
10. Oi, S., Inamasu, M., and Yasunobu, K. T. (1970) *Biochemistry 9*, 3378−3383.
11. Cleland, W. W. (1979) *Methods Enzymol. 63*, 103−138.
12. Su, Q. (1999) Ph.D. Thesis, University of California, Berkeley, CA.
13. Whittaker, J. W., Orville, A. M., and Lipscomb, J. D. (1990) *Methods Enzymol. 188*, 82−89.
14. Parsons, M. R., Convery, M. A., Wilmot, C. M., Yadav, K. D., Blakeley, V., Corner, A. S., Phillips, S. E., McPherson, M. J., and Knowles, P. F. (1995) *Structure 3*, 1171−1184.
15. Kumar, V., Dooley, D. M., Freeman, H. C., Guss, J. M., Harrey, I., McGuirl, M. A., Wilce, M. C. J., and Zubak, V. M. (1996) *Structure 4*, 943−955.
16. Wilce, M. C. J., Dooley, D. M., Freeman, H. C., Guss, J. M., Matsunami, H., McIntire, W. S., Ruggiero, C. E., Tanizawa, K., and Yamaguchi, H. (1997) *Biochemistry 36*, 16116−16133.
17. Battino, R. (1981) *Solubility Data Series*, Vol. 7, International Union of Pure and Applied Chemistry, Research Triangle Park, NC.
18. Engelman, D. M., Steitz, T. A., and Goldman, A. (1986) *Annu. Rev. Biophys. Biochem. 15*, 321−353.
19. Palecz, B. (2002) *J. Am. Chem. Soc. 124*, 6003−6008.

20. Hevel, J. M., Mills, S. A., and Klinman, J. P. (1999) *Biochemistry 38*, 3683−3693.
21. Chothia, C. (1975) *Nature 254*, 304−308.
22. Murcus, R. A., and Sutin, N. (1985) *Biochim. Biophys. Acta 811*, 265−322.
23. Mure, M., and Klinman, J. P. (1993) *J. Am. Chem. Soc. 115*, 7117−7127.
24. Kuznicki, S. M., Bell, V. A., Nair, S., Hillhouse, H. W., Jacubinas, R. M., Braunbarth, C. M., Toby, B. H., and Tsapatsis, M. (2001) *Nature 412*, 720−724.
25. Saunders, M., Jimenez-Vasquez, H. A., and Khong A. (1996) *J. Phys. Chem. 100*, 15968−15971.

BI0204591